Comprehending the Bending: A Comparison of Different Test Setups for Measuring the Out-of-Plane Flexural Rigidity of a UD Fabric

Krogh, Christian; Broberg, Peter Hede; Kepler, Jørgen; Jakobsen, Johnny

Published in:
Key Engineering Materials

DOI (link to publication from Publisher):
10.4028/p-r883x4

Publication date:
2022

Document Version
Publisher's PDF, also known as Version of record

Key Engineering Materials
ISSN: 1662-9795, Vol. 926, pp 1257-1267
doi:10.4028/p-r883x4

Submitted: 2021-12-06
Revised: 2022-01-13
Accepted: 2022-02-18
Online: 2022-07-22

Comprehending the Bending: A Comparison of Different Test Setups for Measuring the Out-of-Plane Flexural Rigidity of a UD Fabric

Christian Krogh[1,a*], Peter Hede Broberg[1,2,b], Jørgen Kepler[1,c], and Johnny Jakobsen[1,d]

[1]Department of Materials and Production, Aalborg University, Fibigerstraede 16, Aalborg, Denmark

[2]CraCS Research group, Aalborg University, Fibigerstraede 16, Aalborg, Denmark

[a]ck@mp.aau.dk, [b]phb@mp.aau.dk, [c]jk@mp.aau.dk, [d] joj@mp.aau.dk

Keywords: Fabrics, UD NCF, Out-of-Plane Bending Test

Abstract. To simulate the forming process of a unidirectional (UD) glass fiber non-crimp fabric (NCF) for wind turbine blades, the fabric material needs to be characterized. In this way, input to the material model of the simulation can be generated. One important deformation to characterize is the out-of-plane bending. A number of test setups have been described in the literature but it is not clear which setup is more appropriate for the UD NCF under consideration. Therefore, five different out-of-plane bending test setups are compared and discussed, namely Peirce's cantilever test (with an inclined plane), the free-hanging cantilever test, a vertical cantilever test, a rotary rheometer bending test and a buckling test. For the latter an inverse modeling approach is developed. The test results shows that similar flexural rigidities can be computed from the different test setups but that some values are sensitive to the parameters used in the data processing techniques.

Introduction

Wind turbine blades are made using a fiber reinforced polymer material with glass fibers being the predominant reinforcement material. During the production process of the blades, plies of stitched so-called non-crimp fabric (NCF) are placed in the blade mold and subsequently cured with the resin. A part of the the NCF plies are unidirectional (UD), i.e. with all the fibers aligned in the same direction. To simulate the handling, i.e. draping and consolidation of such UD NCF plies, see e.g. Broberg et al. [1], the different deformation mechanisms must first be characterized. This study focuses on the out-of-plane flexural rigidity or bending stiffness.

The characterization of the bending stiffness of fabrics has been studied extensively. In general, the out-of-plane deformation of fabrics does not strictly follow the classical Bernoulli-Euler beam theory due to transverse shear from fiber sliding. The term *bending stiffness* is, however, still used as the relation between the moment, M and the curvature κ of the fabric's centerline [2]. Here, the quantity *bending stiffness per unit width*, B_w is used:

$$M = B_w \, w \, \kappa. \tag{1}$$

In the expression w is the specimen width. For the classical beam theory $B_w \, w = EI$, i.e. is equal to the product of Young's modulus and the area moment of inertia.

A simple test setup for measuring the bending stiffness of fabrics is the Peirce cantilever test (PCT) [3], which is now the basis for the ASTM standard D1388. It was developed in the 1930's and is based on a strip of fabric cantilevered under its own weight above an inclined plane. Based on the angle of the plane and the overhang length when the fabric tip touches the plane, a constant bending stiffness can be estimated.

An extension of the Peirce method, the free-hanging cantilever test (FCT), i.e. without the inclined plane, was developed by Clapp et al. [4]. The idea is to capture the deformed shape of the fabric from a digital image of the specimen and by means of curve fitting and a static analysis compute the moment and curvature along the length of the specimen. See also the more recent studies in [5, 6]. A vertical cantilever test (VCT) was proposed by Soteropoulos et al. [7] to alleviate issues with twisting of the

specimen's free end. The deflection was created by a mass tied to a string, which was attached to the unclamped end of the specimen. A pulley ensured that the pulling force on the specimen was horizontal (see also the study in [8]). The setup was extended by Alshahrani et al. [9] in the form of an actuator and a load cell for creating the specimen deflection and recording the applied force. This setup can for instance be used to measure stress relaxation in the specimen.

A second type of test involves the imposing of an out-of-plane deformation on the specimen by means of a rotation. The bending test from the Kawabata evaluation system (KES) is a standardized way of performing such a rotational test. The two ends of a fabric strip are installed in a stationary and moving clamp, respectively. Sliding is possible in the stationary clamp. The moving clamp describes a circular motion at a fixed rate whereby the bending moment vs. curvature can be measured. The test does, however, require a specific test machine which is costly [10].

The principle of the Kawabata bending test was applied in the test setup by Sachs and Akkerman [2] in which a rotational rheometer and a special fixture was used to impose the rotation on the specimen. The test was denoted the rheometer bending test (RBT). See also the study by Poppe et al. [11] that features a comparison between the RBT and the FCT for a low viscous infiltrated fabric. The authors reported that the RBT in general would predict a higher bending stiffness than the FCT which among others was explained by sliding friction of the specimen in the moving clamp.

Yet another type of test setup is the buckling test (BT). A strip of the fabric is compressed in a universal testing machine and will thus buckle out of plane. Kocik et al. [12] used the maximum critical force recorded at buckling as the basis for determining the bending stiffness. See also the study by Wang et al. [13] in which a BT was used for comparison with their fabric bending model.

The present study aims to compare the following tests in terms of the applicability to a UD glass fiber NCF: The Peirce cantilever test (PCT), the free-hanging cantilever test (FCT), the vertical cantilever test (VCT), the rheometer bending test (RBT) and the buckling test (BT) which includes the development of an inverse model. The applicability concerns the fabric's rate-independent behavior at room temperature. The remaining contents of the paper include a brief description of the UD glass fiber material, an explanation of the investigated test setups, the obtained results, a discussion of the discrepancies and lastly a conclusion.

Glass Fiber Material

The fabric material tested in this study consists of UD glass fibers in the $0°$-direction, which are stabilized with a layer of $\pm 80°$ glass backing fibers. This configuration is sometimes denoted *quasi-UD*. The areal densities of the UD layer and the backing layer are respectively 1322 g/m^2 and 60 g/m^2. The fibers are held together with a tricot-chain type stitching made from polyester. The total fabric thickness is approximately 1 mm. The fiber mat is coated with a binder material which facilitates pre-consolidation, however the isolated effects of this binder are not investigated here.

Due to the fabric architecture and thickness, the bending stiffness in the $0°$-direction is quite high whereas the bending stiffness in the $90°$-direction, i.e. transverse to the UD rovings is quite weak. This difference will challenge the test methods.

Investigated Test Setups for Measuring the Flexural Rigidity

The out-of-plane bending test setups investigated in this paper are shown schematically in Fig. 1 and discussed in the following. The specimens are tested in the $0°$ direction (indicated with the symbol $\parallel$) and the $90°$ direction (indicated with the symbol $\perp$). The preliminary tests suggest that there is a small difference between having the UD side or backing side in tension during bending. For this comparison all the results are obtained with the UD side in tension. It was also observed that the bending stiffness would decrease after a specimen had been bent once. For this reason three repetitions of each test were made, each with a pristine, unbent specimen. Although the results to some extent could be specimen length dependent, particularly for PCT, only one length was investigated for each test. The lengths of

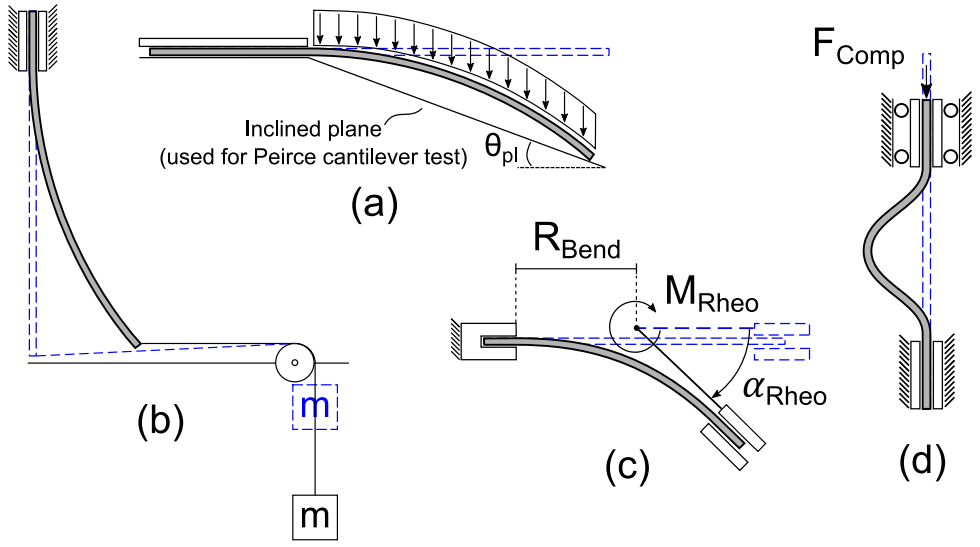

Fig. 1: Test setups for measuring the out-of-plane bending stiffness of fabrics investigated in this paper: (a) Cantilever test (setup used for Peirce cantilever test and free-hanging cantilever test), (b) Vertical cantilever test. (c) Rheometer bending test, top view and (d) Buckling test.

Table 1: Specimen data used for the different test setups.

	PCT + FCT	**VCT**	**RBT**	**BT**
Unclamped length	∥: 250 mm ⊥: 40 mm	200 mm	70 mm	70 mm
Width	50 mm	50 mm	50 mm	40 mm
Imposed load or deformation	13.6 N/m^2 (gravity)	∥: 0.12838 N ⊥: 0.00453 N (tipload)	0° - 90° at 4.5 °/s (rotation)	30 mm at 20 mm/min (displacement)

the PCT, FCT, VCT and BT specimens were chosen to obtain a suitable deflecting shape. The length of the RBT specimen was chosen to match the fixture. The specimen data from the the different tests are provided in Table 1.

Peirce cantilever test. A schematic of the Peirce cantilever test (PCT) is shown in Fig. 1(a). In the test, the sample is cantilevered under its own weight such that it makes contact with the inclined plane. Based on the overhang length, l, and the angle of the inclined plane, θ_{pl} the bending stiffness per unit width, B_w (constant) can be computed [3]:

$$B_w^{\mathrm{PCT}} = \frac{W_a\, l^3}{8\, \tan(\theta_{\mathrm{pl}})} \cos(\theta_{\mathrm{pl}}/2). \tag{2}$$

Here W_a is the weight per unit area (N/m^2). The factor $\cos(\theta_{\mathrm{pl}}/2)$ was empirically introduced by Peirce as a correction for large angles. While the Peirce cantilever test is simple and easy to perform the assumption of a constant bending stiffness, i.e. a linear moment-curvature relation can be a crude approximation for some fabrics [14].

Free-hanging cantilever test. The setup of the free-hanging cantilever test (FCT) is similar to that of the Peirce test in Fig. 1(a), except that the inclined plane is absent. The data processing follows the description by Liang et al. [6]: Using a digital camera and a neutral background with high contrast to the specimen (here: black) the deformed specimen is recorded at the steady state. Using image processing techniques, the image is smoothed and the midline of the specimen is identified. Next, a

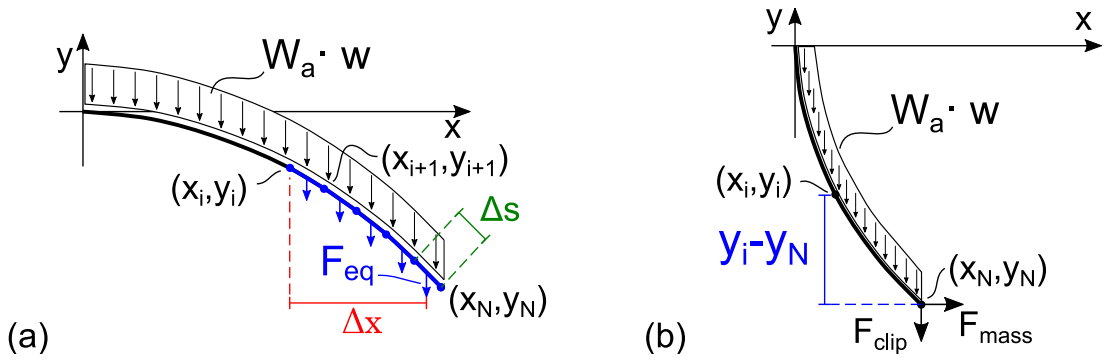

Fig. 2: Computation of bending moment along the arclength of the specimen: (a) Free-hanging cantilever test with F_{eq}, Δx, and Δs shown for $k = N - 1$. (b) Vertical cantilever test.

spline curve, $C(x)$ can be fitted and the absolute curvature can be computed as:

$$\kappa = \left| \frac{C''(x)}{[1 + C'(x)^2]^{3/2}} \right| . \tag{3}$$

Here the primes denote differentiation. The moment can be obtained from a static analysis as shown in Fig. 2(a). The moment contribution from the selfweight, $W_a\, w$, can be computed by integration along the arclength of the fabric. In a discrete numerical implementation the integral can be replaced with a sum so that the moment at the ith point along the arclength, (x_i, y_i), becomes:

$$M_i^{\text{FCT}} = \sum_{k=i}^{N-1} F_{\text{eq},k}\, \Delta x_k \quad , F_{\text{eq},k} = W_a\, w\, \Delta s_k \qquad , i = 1, 2, ..., N-1. \tag{4}$$

Here, the equivalent force, $F_{\text{eq},k}$, is equal to the product of the line load and the length of the kth line segment Δs_k. This length and the moment arm from (x_i, y_i) to the center of the kth line segment, Δx_k, are respectively computed as:

$$\Delta s_k = \sqrt{(x_{k+1} - x_k)^2 + (y_{k+1} - y_k)^2} \qquad \Delta x_k = x_k - x_i + \frac{x_{k+1} - x_k}{2}. \tag{5}$$

The moment at the Nth point, i.e. at the free end of the fabric is equal to zero. Using this approach a nonlinear moment-curvature relation can be computed. There are, however, some uncertainties related to the image recording and data processing. The test is on the other hand easy to set up.

Vertical cantilever test. In the vertical cantilever test (VCT), the specimen is hung vertically from a fixation as sketched in Fig. 1(b). This setup enables the controlling of the load magnitude and application (rather than controlling the overhang length as in the horizontal cantilever tests) which also makes the specimen less susceptible to twisting. In this study, the load is applied as a mass tied to a string, which is guided through a pulley and attached to the lower end of the specimen. The setup is such that the specimen tip load is horizontal in the deformed configuration. For the $\parallel$ test a paper clip (mass: 3.219 g) was used to attach the string and stabilize the end of the specimen but this was not applied in the $\perp$ test due to the low bending stiffness. The procedure of the optical data acquisition and processing is very similar to the free-hanging, horizontal cantilever test. The only difference is the computation of the moment as seen in Fig. 2(b). If the deflection is small and the areal weight of the fabric is low, the influence of selfweight can possibly be neglected [8]. In this study, it is included and the moment at the ith point along the arclength of the fabric becomes:

$$M_i^{\text{VCT}} = F_{\text{mass}}\, |y_i - y_N| - F_{\text{clip}}\, |x_N - x_i| - \sum_{k=i}^{N-1} F_{\text{eq},k}\, \Delta x_k \qquad , i = 1, 2, ..., N-1. \tag{6}$$

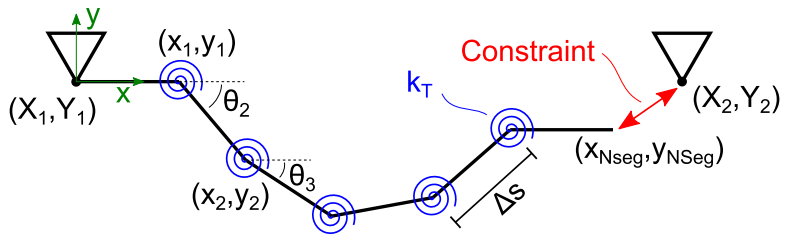

Fig. 3: Discrete elastica (Hencky bar-chain) consisting of six rigid segments connected by torsional springs (actually 50 segments was used). The right support represents the moving crosshead.

And again, the moment at the Nth point, i.e. at the lower end of the fabric, is equal to zero. This test is also quick to set up but suffers from the same uncertainties in the data processing as the FCT. Further, the friction in the pulley can be a source of error at low tip loads.

Rheometer bending test. The rheometer bending test (RBT) relies on a rotational rheometer with a custom-built fixture. A top view is sketched in Fig. 1(c). The fixture enables to clamp the specimen in one end while allowing for sliding in the others (using a spacing of 2 mm). The sliding is necessary because the arclength between the clamps is decreasing during rotation, assuming that the fabric deforms in a circular arc. The rheometer is set up to rotate at a constant angular rate and output the torsional moment vs. the rotation angle. The recorded moment, M_{Rheo} is equivalent to the moment imposed on the specimen (neglecting sliding friction in the clamps) and the constant curvature can be computed based on the rotation angle, α_{Rheo}, as [11]:

$$\kappa^{\text{RBT}} = \frac{\tan\left(\alpha_{\text{Rheo}}/2\right)}{R_{\text{Bend}}}. \tag{7}$$

The bending radius R_{Bend} is equal to half the initial unclamped length. This test requires a rotational rheometer and the custom-built fixture and is thus costly to set up. Ideally, if the sliding friction in the clamps is small the test will give a more direct measure of the moment-curvature relation of the fabric compared to the cantilever-type approaches.

Buckling test. In the buckling test (BT) a strip of the fabric is clamped between the grips of a universal testing machine as sketched in Fig. 1(d). The specimen is then compressed at a constant displacement rate and the compressive force is recorded. The test can be extended with a video or image recording system for subsequent deformation analysis, however, this was not employed in the present study. Assuming that the maximum force recorded is the critical buckling load for a fixed-fixed column with linear elastic material properties, a constant, curvature-independent bending stiffness per unit width can be estimated as [15]:

$$B_w^{\text{BT}} = \frac{F_{\text{Comp}}^{\max} L^2}{4\pi^2} \frac{1}{w}. \tag{8}$$

Here L is the initial specimen length between the grips. This estimation is based on an ideal column and does therefore not take imperfections into account. It will thus be an underprediction of the maximum bending stiffness because imperfections are unavoidable in the test specimen.

Another, more advanced, data processing method is the use of an inverse modeling approach. That is, to fit the response of a model to the experimental buckling and post-buckling data by adjusting the bending stiffness. Here, it is investigated if a simple model based on a 2D discrete elastica in the form of a *Hencky bar-chain* can be applied. The idea is to divide the unclamped length of the fabric strip into N_{seg} rigid segments which are joined by torsional springs, k_{T} as sketched in Fig. 3. The model is parameterized by the rotation angles of the segments θ_i and to match the clamping boundary conditions, the first and last rotation angles are prescribed to 0. The torsional spring stiffness can be derived from classical beam theory (elaborated later in this section) given the bending stiffness of the

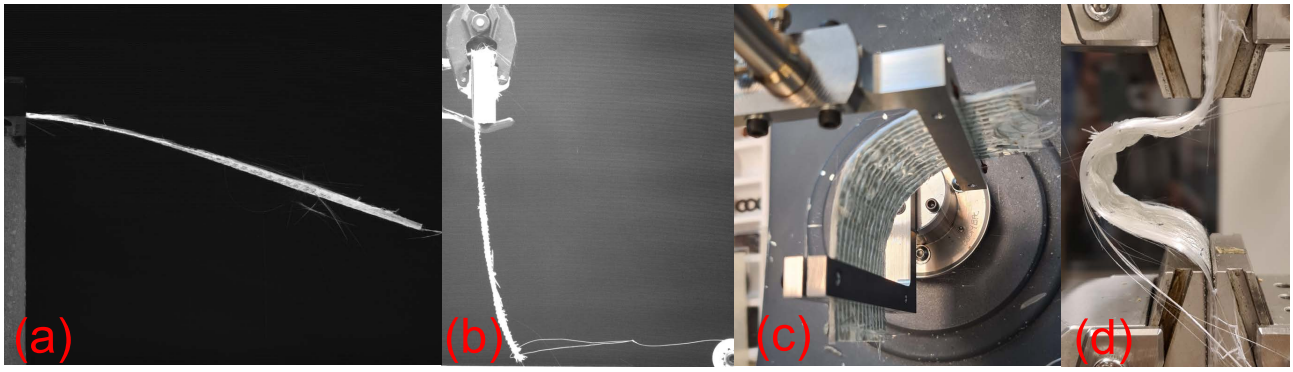

Fig. 4: Deformed test specimens: (a) Free-hanging cantilever test (∥), (b) Vertical cantilever test (⊥), (c) Rheometer bending test (∥), and (d) Buckling test (∥).

beam. Here an expression for the bending stiffness as function of the curvature was created using a three-parameter exponentially decaying function:

$$B(\kappa) = (B_{\text{max}} - B_{\text{min}})\, \mathrm{e}^{-P|\kappa|} + B_{\text{min}}. \tag{9}$$

In the expression, B_{max} and B_{min} control the maximum and minimum bending stiffness, respectively and P controls the decay rate. The equilibrium configuration of the elastica can be found by minimizing the total potential energy subject to the constraint that the end of the last segment, $(x_{\text{Nseg}}, y_{\text{Nseg}})$, must be coincident with the location of the right support, i.e. (X_2, Y_2):

$$\begin{aligned} \underset{\theta}{\text{minimize}} \quad & \Pi = U + \Omega \\ \text{s.t.} \quad & x_{\text{Nseg}} = X_2 \\ & y_{\text{Nseg}} = Y_2. \end{aligned} \tag{10}$$

The total potential energy is the sum of U (the strain energy in the material), and Ω (the potential of externally applied loads). U and Ω are computed by summing the contributions from each segment. The strain energy contribution from the ith segment is the bending strain energy derived from classical beam theory [15] used with the bending stiffness computed from Eq. (9):

$$U_{\text{seg},i} = \frac{B(\kappa_i)\, \Delta\theta_i^2}{2\Delta s_i} \qquad , \Delta\theta_i = \theta_i - \theta_{i-1} \qquad , \kappa_i = \frac{\Delta\theta_i}{\Delta s_i}. \tag{11}$$

That is, a linear elastic beam of length Δs_i (length of segment) bent by the angle $\Delta\theta_i$. The externally applied load is gravity acting in the negative x-direction, whose potential is given as:

$$\Omega_{\text{seg},i} = -W_a\, w\, \Delta s_i\, \Delta x_i. \tag{12}$$

Here Δx_i is the x-distance between the midpoint of the ith segment in its current position and its undeformed position.

Thus, the equilibrium configuration of the elastica can be computed for any value of the right support position, i.e. crosshead position. A sequential quadratic programming (sqp) optimizer with a Lagrangian formulation to handle the equality constraints (MATLAB's *fmincon*) is used together with finite difference gradients. It can be shown, that at the optimum, the Lagrange multipliers of the equality constraints are equal to the reaction forces required to enforce the constraints. Therefore, the Lagrange multiplier corresponding to the first equality constraint can be compared to the measured crosshead force. By choosing a number of points on the recorded force-deflection curve from the buckling test, the differences between the crosshead forces and elastica reaction forces can be minimized using a least squares algorithm (MATLAB's *lsqnonlin*). In this minimization routine, the design variables are the three parameters of the bending stiffness expression in Eq. (9), i.e. B_{max}, B_{min} and P. The

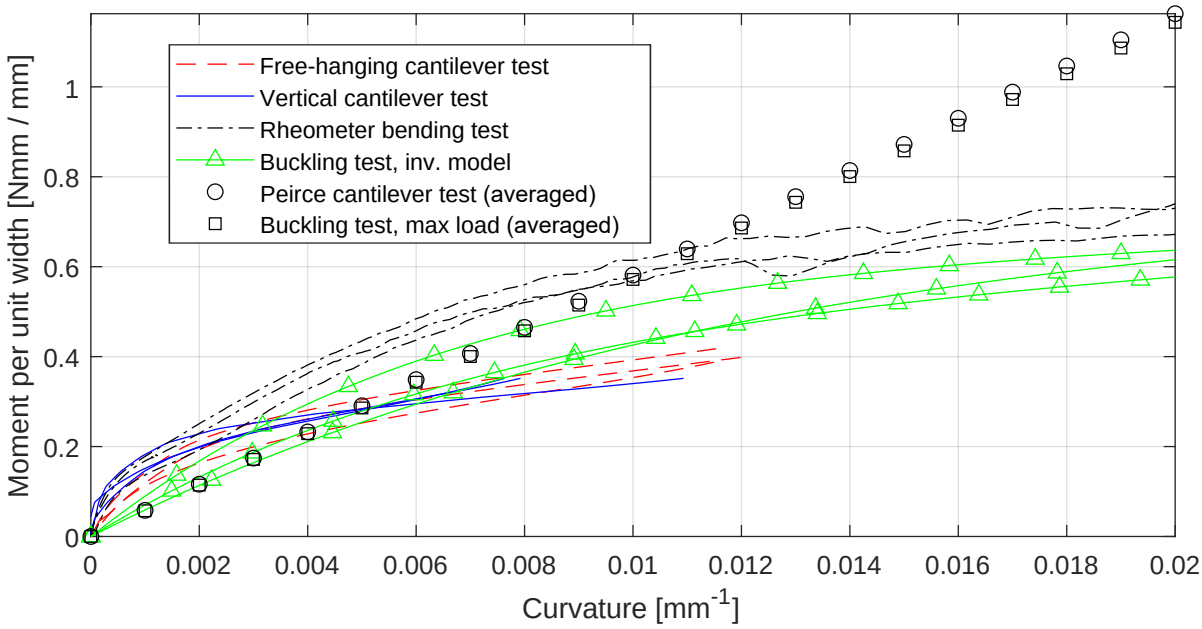

Fig. 5: Moment-curvature results for all test setups for 0° direction (||).

least squares algorithm can be started with a suitable initial guess with basis in the bending stiffness approximated using Eq. (8). The initial guess for the design variables are $B^0_{\max} = B^{\mathrm{BT}}_w$, $B^0_{\min} = 0.5\, B^{\mathrm{BT}}_w$ and $P^0 = 10^{-6}$. Upper and lower bounds ensure that the bending stiffness always remains greater than zero. A total of 50 segments were used for the elastica model and six points on the force-displacement curve was chosen for the least squares minimization. The least squares solution was found in a couple of minutes on a standard laptop.

Results

Typical deformed specimens from the experiments are presented in Fig. 4. It can be seen how a general challenge with conducting the tests was loose fibers.

The results of the 0°-direction (||) specimens are presented in Fig. 5 as the width-normalized moment vs. curvature. It can be seen that the free-hanging cantilever test (FCT) and the vertical cantilever test (VCT) yield results that agree reasonably well. Further, the FCT and the VCT curves are similar in shape to the rheometer bending test (RBT) curve but a good agreement is only seen until a curvature of around 0.002 mm^{-1}. At a curvature of 0.01 mm^{-1}, the width-normalized moment is approximately 50% higher for the RBT compared to the FCT and VCT. Similar discrepancies were observed by Poppe et al. [11] who gave two main explanations: 1) Sliding friction in the clamps of the RBT and 2) a reduced specimen thickness of the FCT and VCT near the fixation due to the clamping force. It should be remarked, though, that for FCT, VCT and RBT, the slopes, i.e. bending stiffnesses cf. Eq. (1), tend towards very similar values at higher curvatures.

The Peirce cantilever test (PCT) assumes a constant bending stiffness and is thus yields a linear moment-curvature relation. It appears as a “best fit” to the FCT curves. The buckling test (BT) has two results in Fig. 5: A constant bending stiffness estimated based on the maximum recorded load and the inverse modeling approach. The former is similar to the PCT results but it should be noted that the buckling response is very sensitive to the imperfections which means that the same will apply to the computed stiffness. The latter, i.e. the inverse modeling approach, predicts a nonlinear moment-curvature relation which for curvatures larger than 0.002 mm^{-1} is similar to the RBT in shape but slightly lower in value. These BT curves are based on the first part of the post-buckling response as seen in Fig. 6 as this was found to yield the lowest residuals in the least-squares minimization. The

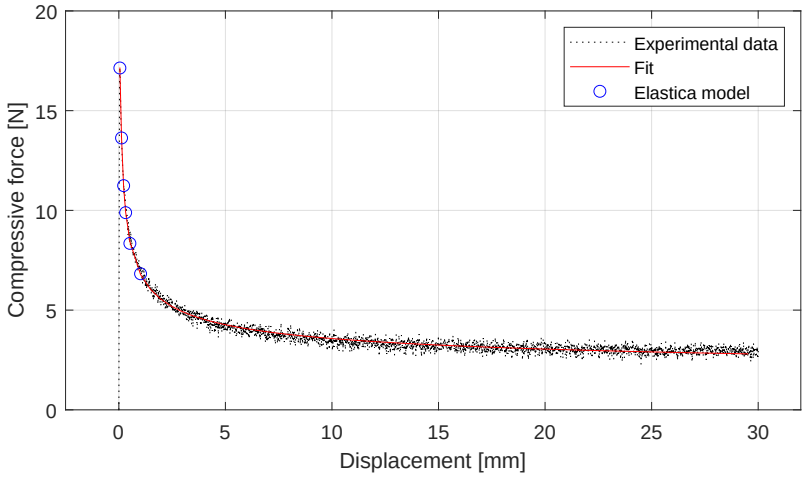

Fig. 6: Compressive force vs. displacement for a specimen in the buckling test. A power law was fitted to the data from the maximum force to the end of the test. The blue circles indicate the reaction forces of the least-squares minimized elastica solutions.

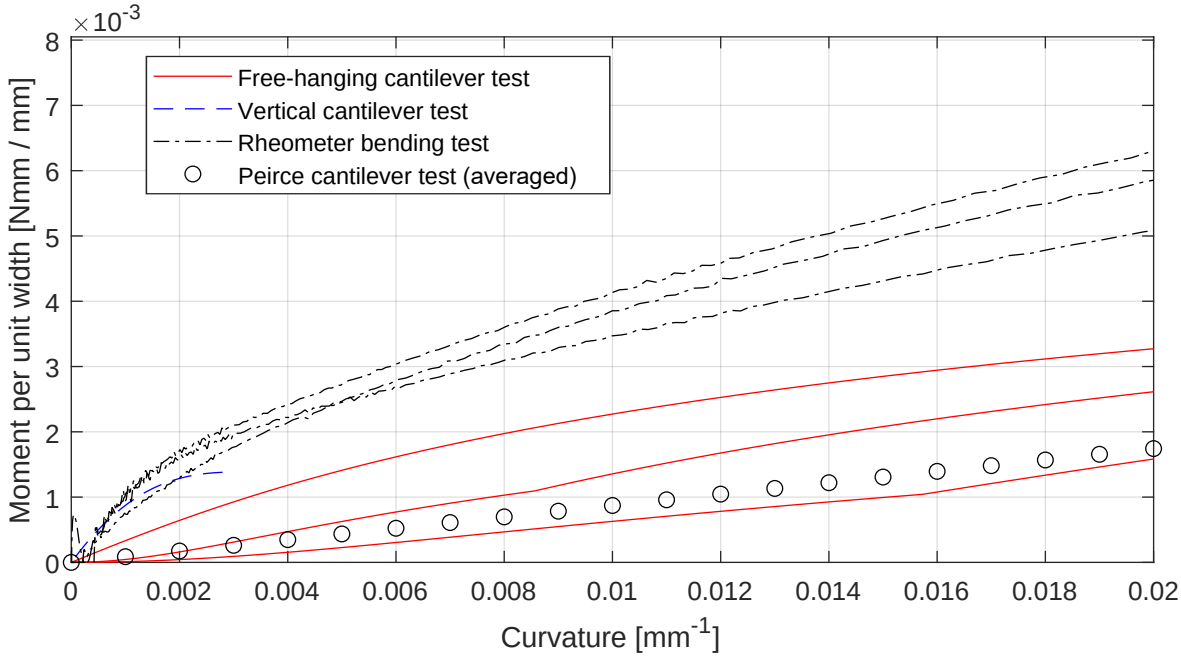

Fig. 7: Moment-curvature results for all applicable test setups for 90° direction (⊥).

curvatures of the BT specimens in this range are also adequate in magnitude for comparison with the other tests.

The results of the 90°-direction (⊥) specimens are presented in Fig. 7. Due to the very low bending stiffness of the fabric in this direction, the buckling test (BT) was not applied because the specimen would buckle under its own weight. The vertical cantilever test (VCT) did not perform well either. The reason is the combination of the very low bending stiffness and the high areal weight of the fabric. A mass of only 0.5 grams would give a maximum horizontal deflection of approximately 20 mm. However, at this deflection, the moment contribution from gravity has the same order of magnitude as the moment contribution from the tip load. Further, the moment and curvature curves were not monotonically increasing from the tip towards the fixation. Therefore only a part of a single specimen curve has been included in the results comparison.

The results of the free-hanging cantilever test (FCT) and the rheometer bending test (RBT) again predict a similar trend, with the RBT curves being higher in magnitude. There is a large degree of uncertainty with the FCT results because the specimens only were 40 mm in length. This was found to be the maximum length that would produce a reasonable deflection and curvature but it means a low signal-to-noise ratio during the image processing and curve fitting. The Peirce cantilever test is again similar to the FCT curves.

Discussion

The previous section has presented results for specimens cut in the 0° (∥) and 90°-direction (⊥). For the former the results were fairly similar whereas for the latter there were large discrepancies. In principle, the only test that is applicable to both ∥ and ⊥ specimens while producing repeatable results was the rheometer bending test (RBT). The test can also conveniently be extended with rate and temperature control using the environmental chamber for the rheometer. The potential uncertainties with the sliding friction, however, have to be investigated further. An optical measure could also be used to check that the specimen deforms with constant curvature as assumed in the data processing.

The free-hanging cantilever test (FCT) and the vertical cantilever test (VCT) gave similar as well as repeatable results with the ∥ specimens. With the ⊥ specimens, the results were less repeatable and thus the comparison is more difficult. While the vertical arrangement of the specimen did result in less twisting and this setup easier can account for rate dependency and stress relaxation [9], it is slightly more cumbersome to set up. For both the FCT and the VCT a proper "load" must be found that will result in a reasonable deflection and curvature. For the FCT this means adjusting the unclamped length whereas for the VCT in this basic setup, this means changing the mass. The specimen length can of course also be adjusted and the use of a shorter specimen could maybe improve the ⊥ VCT results in Fig 7. For both the FCT and VCT there are large uncertainties in the image processing and curve fitting steps of the data processing. It was found that especially the computed curvature (i.e. a function of the 2nd derivative cf. Eq (3)) is highly sensitive to the input parameters of smoothing and curve fitting.

As is evident from the comparison of the results in Fig. 5 and 7, the moment-curvature relation is nonlinear. The bending stiffness, i.e. slope, decreases with an increase in curvature. This phenomenon can for the ∥ specimens be explained by micro-buckling of the UD rovings between the stitches which was observed during the test for large curvatures and also previously reported on a UD carbon fiber prepreg [13]. The FCT, VCT and RBT agree well for low curvatures which is also their region of highest fidelity: For FCT and VCT the low curvatures are measured furthest away from the fixation and for the RBT, the low curvatures occur in the beginning of the test where sliding friction is negligible. For larger curvatures, the inverse approach with the buckling test (BT) could be a reasonable approximation because the sensitivity to the imperfections vanish when moving away from the maximum load, i.e. during post-buckling.

The Peirce cantilever test (PCT) was also applicable to both ∥ and ⊥ specimens but due to the nonlinearity of the moment-curvature relation, the PCT will only be an approximation. Using the maximum compressive force from the Buckling test (BT) to compute a constant stiffness, gave a reasonable approximation similar to the PCT for ∥ specimens. Another applicability of the BT would be a validation case because the specimen will experience a wide range of curvatures from negative to positive values.

Conclusion

This paper has investigated five different test setups for measuring the out of plane bending of a UD fabric: the Peirce cantilever test, the free-hanging cantilever test, the vertical cantilever test, the rheometer bending test and the buckling test. For the latter, an inverse modeling approach was devel-

oped which showed promise. The test specimens were cut in the 0° and 90° directions thus presenting, respectively, high and low bending stiffnesses to be measured.

The comparison of the results showed a fair degree of similarity for the 0°-specimens but a relatively high variability for the 90°-specimens. Thus, the low bending stiffness and high areal weight was a challenge. Overall, the rheometer bending test performed most consistently but sliding friction in the clamps is an un-quantified source of error. In addition the test relies on costly equipment. Overall, the free-hanging cantilever test is a promising simple and low-cost setup but the uncertainties in the data processing must be addressed. With an objective and consistent data processing approach, this test should be able to accurately characterize the bending stiffness of the UD glass fiber fabric in question.

Acknowledgements

This study was completed as part of the MADEBLADES research project supported by the Energy Technology Development and Demonstration Program, Grant no. 64019-0514.

References

[1] P. H. Broberg, C. Krogh, E. Lindgaard, and B. L. V. Bak. Simulation of wrinkling during forming of binder stabilized UD-NCF preforms in wind turbine blade manufacturing. In *Proceedings of the 25th ESAFORM conference*, Braga, Portugal, 2022.

[2] U. Sachs and R. Akkerman. Viscoelastic bending model for continuous fiber-reinforced thermoplastic composites in melt. *Composites Part A: Applied Science and Manufacturing*, 100:333–341, sep 2017.

[3] F. T. Peirce. 26—The "handle" of cloth as a measurable quantity. *Journal of the Textile Institute Transactions*, 21(9):T377–T416, jan 1930.

[4] T. G. Clapp, H. Peng, T. K. Ghosh, and J. W. Eischen. Indirect Measurement of the Moment-Curvature Relationship for Fabrics. *Textile Research Journal*, 60(9):525–533, 1990.

[5] E. de Bilbao, D. Soulat, G. Hivet, and A. Gasser. Experimental Study of Bending Behaviour of Reinforcements. *Experimental Mechanics*, 50(3):333–351, mar 2010.

[6] B. Liang, P. Chaudet, and P. Boisse. Curvature determination in the bending test of continuous fibre reinforcements. *Strain*, 53(1):e12213, feb 2017.

[7] D. Soteropoulos, K. Fetfatsidis, J. A. Sherwood, and J. Langworthy. Digital method of analyzing the bending stiffness of non-crimp fabrics. In *AIP Conference Proceedings*, volume 1353, pages 913–917. AIP Publishing, apr 2011.

[8] L. M. Dangora, C. J. Mitchell, and J. A. Sherwood. Predictive model for the detection of out-of-plane defects formed during textile-composite manufacture. *Composites Part A: Applied Science and Manufacturing*, 78:102–112, 2015.

[9] H. Alshahrani and M. Hojjati. A new test method for the characterization of the bending behavior of textile prepregs. *Composites Part A: Applied Science and Manufacturing*, 97:128–140, 2017.

[10] S. V. Lomov, I Verpoest, M Barburski, and J Laperre. Carbon composites based on multiaxial multiply stitched preforms. Part 2. KES-F characterisation of the deformability of the preforms at low loads. *Composites Part A: Applied Science and Manufacturing*, 34(4):359–370, 2003.

[11] C. Poppe, T. Rosenkranz, D. Dörr, and L. Kärger. Comparative experimental and numerical analysis of bending behaviour of dry and low viscous infiltrated woven fabrics. *Composites Part A: Applied Science and Manufacturing*, 124:105466, sep 2019.

[12] M. Kocik, W. Zurek, I. Krucinska, J. Geršak, and J. Jakubczyk. Evaluating the bending rigidity of flat textiles with the use of an instron tensile tester. *Fibres and Textiles in Eastern Europe*, 13(2):31–34, 2005.

[13] J. Wang, A. C. Long, and M. J. Clifford. Experimental measurement and predictive modelling of bending behaviour for viscous unidirectional composite materials. *International Journal of Material Forming*, 3(SUPPL. 2):1253–1266, sep 2010.

[14] P. Boisse, J. Colmars, N. Hamila, N. Naouar, and Q. Steer. Bending and wrinkling of composite fiber preforms and prepregs. A review and new developments in the draping simulations. *Composites Part B: Engineering*, 141:234–249, jan 2018.

[15] J. M. Gere and B. J. Goodno. *Mechanics of Materials*, volume 7. Cengage Learning, Stamford, CT, USA, 2008.